Dalton Transactions

COMMUNICATION

View Article Online
View Journal | View Issue

Cite this: *Dalton Trans.*, 2016, **45**, 17602

Received 20th September 2016, Accepted 14th October 2016

DOI: 10.1039/c6dt03659g

www.rsc.org/dalton

$K_3[Mo_2(SNO5)_4Cl]_3[Mo_2(SNO5)_4]$: the first example of a heterometallic extended metal atom node (HEMAN)†

Brian S. Dolinar,[a] Stosh A. Kozimor[b] and John F. Berry*[a]

We present the synthesis, structure, and electrochemistry of $K_3[Mo_2(SNO5)_4Cl]_3[Mo_2(SNO5)_4]$ (1, HSNO5 = monothiosuccinimide), the first example of a heterometallic extended metal atom node (HEMAN). The HEMAN consists of two perpendicular, intersecting lines of metal atoms formed by three $[Mo_2(SNO5)_4Cl]^-$ units and one $[Mo_2(SNO5)_4]$ unit tethered together by K^+ ions.

Extended metal atom chains (EMACs, Chart 1) and their heterometallic analogs (HEMACs) are multimetallic coordination compounds consisting of three or more linked metal atoms held together in a row by supporting ligands. These multimetallic species are of particular interest for advancing technologies associated with one-dimensional wires and transistors,[1] in the fabrication of molecule-scale logic gates, and as well-defined molecular wire junctions.[2] Since the discovery of the first EMAC, $Ni_3(dpa)_4Cl_2$ (dpa = 2,2′-dipyridylamide),[3] many synthetic advances have provided a novel family of linear-trimetallic EMAC and HEMAC compounds.[4] While these discoveries have advanced the implementation of the EMACs and HEMACs in molecular wires,[1] these technologies would significantly benefit from even more sophisticated EMAC and HEMAC architectures. Of particular interest is the extended metal atom node (EMAN), shown in Chart 1, in which two metal atom chains cross each other. Accessing such scaffolds would provide potential access to molecular wire junctions that link two-dimensional networks of EMACs or HEMACs. Herein, we report the first assembly of a potential EMAN building block.

Exploration of the monothiosuccinimide ligand (HSNO5, Scheme 1) has led us to synthesize a variety of heterotrimetallic EMACs consisting of a dimolybdenum unit paired with a heterometal selected from the alkali metals (Li^+, Na^+), alkaline earth metals (Ca^{2+}, Sr^{2+}), Group III (Y^{3+}), or the lanthanides.[4o,s] Unlike in EMACs supported by equatorial dpa ligands, which consistently feature 3-center metal–metal σ bonds, the heterometal of the $SNO5^-$ compounds is farther away from the $[Mo_2]^{4+}$ unit and influences its Lewis acidity and redox properties in a purely Coulombic manner. An interesting consequence of the extra distance between the heterometal and the $[Mo_2]^{4+}$ unit is that the coordination sphere of larger heterometals is not fully saturated by the four $SNO5^-$ ligands. This steric unsaturation offers potential for the self-assembly of supramolecular structures. In contrast to our results with Li^+, in which a discrete heterotrimetallic M⋯Mo≡Mo compound is produced, we show here that the larger K^+ ion leads to the self-assembly of the 11-core heterometallic EMAN

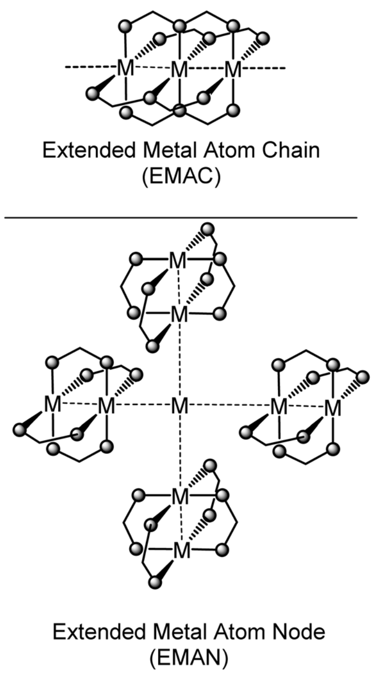

Chart 1 The general structures of (a) EMACs and (b) EMANs.

[a]*Department of Chemistry, University of Wisconsin-Madison, 1101 University Avenue, Madison, WI, 53706, USA. E-mail: berry@chem.wisc.edu*

[b]*Inorganic Isotope and Actinide Chemistry Group, Los Alamos National Laboratory, Los Alamos, NM, 87545, USA*

† Electronic supplementary information (ESI) available: Experimental section, and crystallographic data. CCDC 1497513 and 1497514. For ESI and crystallographic data in CIF or other electronic format see DOI: 10.1039/c6dt03659g

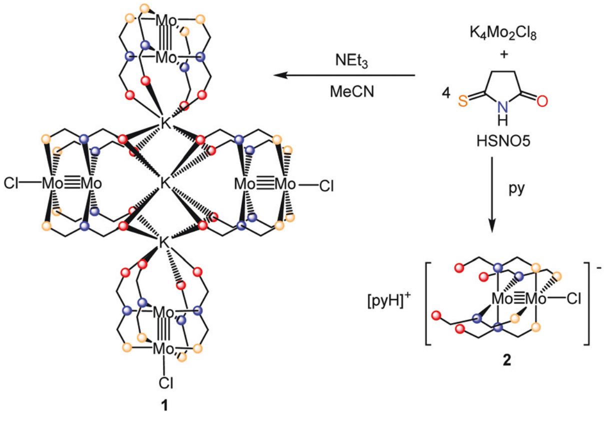

Scheme 1 The synthetic route to **1** and **2**.

(HEMAN) $K_3[Mo_2(SNO5)_4Cl]_3[Mo_2(SNO5)_4]$ (**1**) in MeCN, in which four Mo_2 units are connected to a central core containing three K^+ ions.

The reactivity between quadruply-bonded $[Mo_2]^{4+}$ complex $K_4Mo_2Cl_8$ and HSNO5 offers access to two products based on the solvent used in the reaction (Scheme 1). For instance, when $K_4Mo_2Cl_8$ is reacted with HSNO5 with MeCN as the solvent, the desired HEMAN, **1**, is produced. However, when more coordinating solvents are used, *e.g.* pyridine, K^+ is not retained in the final product and $[pyH][4,0\text{-}Mo_2(SNO5)_4Cl]$ (**2**) forms (*vide infra*). Both **1** and **2** attain the 4,0 configuration of $SNO5^-$ ligands about the $[Mo_2]^{4+}$ core, in which all four ligands are oriented in the same direction with respect to the Mo≣Mo axis. These observations are consistent with previous reports that the presence of a Lewis acid in the reaction mixture facilitates formation of the 4,0 regioisomer as opposed to the *trans*-2,2 or *cis*-2,2 regioisomers favored in the absence of a Lewis acid.[4o,5]

The crystal structure of **1** is shown in Fig. 1. The compound crystallizes as two-symmetry independent half-molecules of **1** in the space group $P\bar{1}$. Each half-molecule occupies a crystallographic inversion center and each full-molecule consists of three $[Mo_2(SNO5)_4Cl]^-$ units and one $Mo_2(SNO5)_4$ unit. The chloride on the axial $Mo_2(SNO5)_4$ unit is disordered between the two sites with a 50% occupancy at each site, giving rise to the crystallographic inversion symmetry. The most defining feature of this compound is the two perpendicular, intersecting lines of metal atoms that is created. The four $[Mo_2]^{4+}$ units are held together by three K^+ ions lying along a non-crystallographic C_2 symmetry axis of the pseudo-C_{2v}-symmetric molecule. The three K^+ ions, eight Mo atoms, and three Cl^- ions reside in a non-crystallographic mirror plane that bisects the complex. Each of the $[Mo_2]^{4+}$ components is bonded to four $SNO5^-$ ligands situated in a 4,0-paddlewheel arrangement. The $SNO5^-$ ligands on each of the axial $[Mo_2]^{4+}$ units (parallel to the principal axis) reside in the molecular mirror planes. Each of the $SNO5^-$ ligands on the two equatorial $[Mo_2]^{4+}$ units (perpendicular to the principal axis) are rotated out of the plane by approximately 45° to avoid a steric clash between the

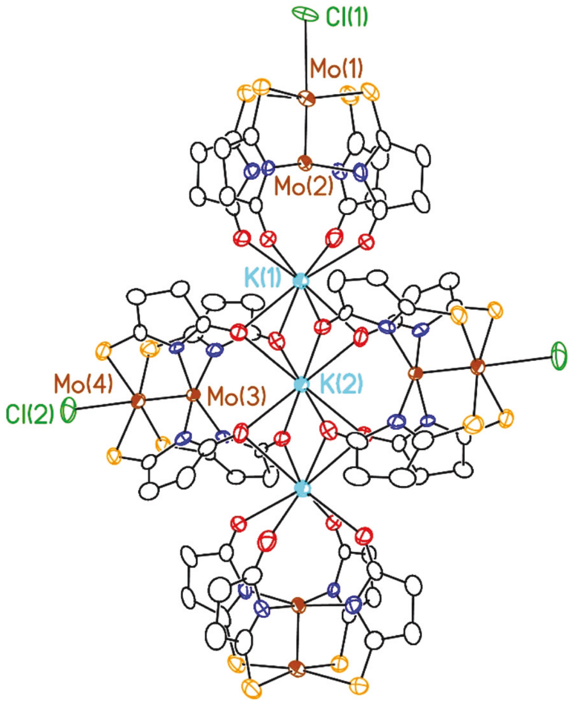

Fig. 1 The X-ray crystal structure of **1**. All atoms are drawn as 50% thermal probability ellipsoids. Brown atoms denote Mo, green atoms denote Cl, sky blue atoms denote K, orange atoms denote S, red atoms denote O, dark blue atoms denote N, and black atoms denote C. All hydrogen atoms are omitted for clarity.

$SNO5^-$ ligands of the axial $[Mo_2]^{4+}$ units. There are three K^+ ions coordinated by eight O atoms from the $SNO5^-$ ligands. These oxygen atoms form a cube around the central K^+ cation and square anti-prisms around the other two K^+ ions.

Relevant bond distances for both the axial and equatorial $[Mo_2]^{4+}$ components of **1** are listed in Table 1. For both the axial and equatorial $[Mo_2]^{4+}$ components, the Mo≣Mo quadruple bond is 2.14 Å, which is elongated compared with the average quadruple bonded Mo≣Mo distance.[6] This elongation is consistent with other $4,0\text{-}[Mo_2(SNO5)_4Cl]^-$ variants,[4o,s] and has been attributed to the donation of electron density from the axial Cl^- ligand to the $[Mo_2]^{4+}$ σ* and π* orbitals. The $K\cdots Mo_2$ distance is shorter for the axial component than it is for the equatorial component (3.938[2] and 4.091[1] Å, respectively), likely due to the difference in K^+ coordination geo-

Table 1 Important crystallographic bond distances for **1**

d(Mo≣Mo) (Å)	2.138[1] (ax)
	2.144[1] (eq)
d(Mo–S) (Å)	2.497[1] (ax)
	2.494[1] (eq)
d(Mo–N) (Å)	2.161[3] (ax)
	2.150[3] (eq)
d(Mo_2–Cl) (Å)	2.733[2] (ax)
	2.670[2] (eq)
d($K\cdots Mo_2$) (Å)	3.938[2] (ax)
	4.091[1] (eq)

metry. This observation is further supported by the shorter K–O distances in the axial $[Mo_2]^{4+}$ units as compared with those of the equatorial $[Mo_2]^{4+}$ units. These K···Mo_2 distances are significantly longer than the heterometallic separations in either the Na^+ or Li^+ analogs (3.505(2) Å and 3.075(5) Å, respectively), primarily due to the larger ionic radius of K^+ (1.52 Å).[7] The Mo_2–Cl bond distances of the axial $[Mo_2]^{4+}$ units are longer than those of the equatorial $[Mo_2]^{4+}$ units (2.733[2] Å and 2.670[2] Å, respectively). This difference is attributable to the packing arrangement of **1** in the crystal structure (ESI, Fig. S3†). The chlorides on the equatorial $[Mo_2]^{4+}$ units point directly into pockets in the structure of neighboring molecules of **1**, whereas the axial Cl^- ligands are not constrained by these interactions.

Cyclic voltammetry was performed between 750 mV and −850 mV *vs.* Fc/Fc^+ on a solution of **1** in propylene carbonate with 0.1 M NEt_4PF_6 as the electrolyte (Fig. 2). The cyclic voltammogram exhibits two quasi-reversible oxidation waves. The electrochemical solution was titrated with a 0.1 M solution of KOTf. Over the course of the titration, both of the $[Mo_2]^{4+/5+}$ oxidation waves move to higher potentials, reaching final $E_{1/2}$ potentials of 220 mV and 430 mV *vs.* Fc/Fc^+. These oxidation potentials are similar to those of previously synthesized MMo_2 compounds. The first oxidation potential is in the range of the oxidation potential of $LiMo_2(SNO5)_4Cl$ (319 mV) and the second oxidation potential is in the range of dehalogenated $[LiMo_2(SNO5)_4]^+$ and $[NaMo_2(SNO5)_4]^+$ (446 mV and 480 mV, respectively), indicating that these oxidation potentials correspond to the oxidation potentials of the halogenated and dehalogenated $[Mo_2]^{4+}$ groups of **1**, respectively.[4o,s] The increasing oxidation potential with increasing $[K^+]$ is consistent with previous examples of $[MMo_2(SNO5)_4Cl]^{(n-1)+}$ compounds in which an assembled MMo_2 complex is in equilibrium with demetallated complex in solution.[4o,s] This observation that the compound falls apart in solution is corroborated by the ^1H NMR data collected on the compound in DMSO-d_6 that shows only two signals for the $SNO5^-$ ligand protons (ESI†). The oxidation waves were invariant upon further addition of K^+ to the solution, indicating that these $E_{1/2}$ values correspond to intact

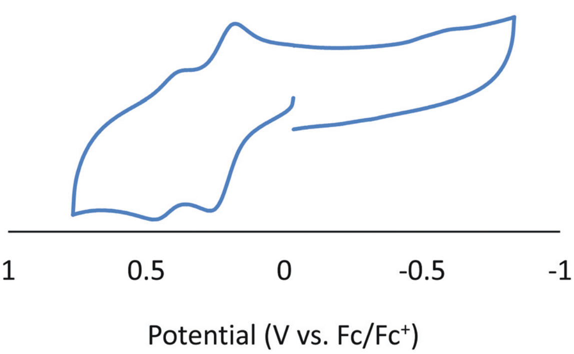

Fig. 2 The cyclic voltammogram of **1**. The sample consisted of 1 mM analyte and 0.1 M NEt_4PF_6 in propylene carbonate. The potential was swept from 0 mV to 750 mV to −850 mV to 0 mV *vs.* Fc/Fc^+ at a rate of 100 mV s^{-1}.

molecules of **1**, however, these data are also consistent with other possible solution compositions, including a mixture of $KMo_2(SNO5)_4Cl$ and $[KMo_2(SNO5)_4]^+$ species.

Our interest in **2** stems from our overarching goal to synthesize unique HEMACs and HEMANs. The open binding pocket on **2** makes it an ideal building block for these complicated molecular architectures, similar to the success we have found with using $pyLiMo_2(SNO5)_4Cl$ (**3**) as a starting material to form HEMACs with a variety of heterometals. Structurally, **2** is somewhat different than **3** (ESI, Fig. S3, Table S2†). While the two compounds have similar Mo≣Mo bond distances the Mo_2–N and Mo_2–S bond distances of **2** (2.155[2] and 2.4870[7] Å, respectively) are considerably longer than those of **3**, but quite close to those of *trans*-2,2-$Mo_2(SNO5)_4$ and *cis*-2,2-$Mo_2(SNO5)_4$.[4o,5] The presence of a third metal in **3** pinches the equatorial $SNO5^-$ ligands into the $[Mo_2]^{4+}$ unit by forming tight M–O bonds. In the absence of a third metal, the equatorial ligands are able to relax to a more optimal bond distance.

In this paper we have described the synthesis and characterization of **1**, the first example of a heterometallic extended metal anode node (HEMAN) structural motif. This structure is similar to that shown in Scheme 1 in that it is composed of four converging $[Mo_2]^{4+}$ subunits held together through coordination to three K^+ ions. Assembly of **1** highlights the diverse structural motifs that can be accessed using the supporting $SNO5^-$ ancillary ligand. The ease with which **1** and **2** were prepared provocatively suggests that a wide variety HEMANs could be accessed for many transition and f-block metals. The planar arrangement of the metal atoms of **1** offers opportunity for future innovation in molecular wires by attachment to planar electrodes or semiconductor surfaces as a molecular logic gates.

Acknowledgements

The authors wish to acknowledge financial support provided under NSF Grant CHE-1300464, and a generous gift from Paul J. Bender (X-ray diffraction). We additionally thank the Office of Science, Heavy Element Chemistry Program at LANL by the Division of Chemical Sciences, Geosciences, and Biosciences, Office of Basic Energy Sciences, U.S. Department of Energy (Kozimor). BSD thanks the LANL Seaborg Institute for a summer research fellowship that contributed to this paper. The authors would like to thank Brian L. Scott for his help in collecting X-ray data.

References

1 (*a*) D.-H. Chae, J. F. Berry, S. Jung, F. A. Cotton, C. A. Murillo and Z. Yao, *Nano Lett.*, 2006, **6**, 165–168; (*b*) V. P. Georgiev, P. J. Mohan, D. DeBrincat and J. E. McGrady, *Coord. Chem. Rev.*, 2013, **257**, 290–298; (*c*) D. DeBrincat, O. Keers and J. E. McGrady, *Chem. Commun.*, 2013, **49**, 9116–9118.

2 (*a*) C. P. Collier, E. W. Wong, M. Belohradský, F. M. Raymo, J. F. Stoddart, P. J. Kuekes, R. S. Williams and J. R. Heath, *Science*, 1999, **285**, 391–394; (*b*) A. Bachtold, P. Hadley, T. Nakanishi and C. Dekker, *Science*, 2001, **294**, 1317–1320; (*c*) Y. Huang, X. Duan, Y. Cui, L. J. Lauhon, K.-H. Kim and C. M. Lieber, *Science*, 2001, **294**, 1313–1317; (*d*) Y. Luo, C. P. Collier, J. O. Jeppesen, K. A. Nielsen, E. Delonno, G. Ho, J. Perkins, H.-R. Tseng, T. Yamamoto, J. F. Stoddart and J. R. Heath, *ChemPhysChem.*, 2002, **3**, 519–525; (*e*) Z. Zong, D. Wang, Y. Cui, M. W. Bockrath and C. M. Lieber, *Science*, 2003, **302**, 1377–1379; (*f*) U. Pischel, *Angew. Chem.*, 2007, **46**, 4026–4040; (*g*) G. de Ruiter and M. E. van der Boom, *Acc. Chem. Res.*, 2011, **44**, 563–573.

3 (*a*) S. Aduldecha and B. Hathaway, *J. Chem. Soc., Dalton Trans.*, 1991, 993–998; (*b*) F. A. Cotton, C. A. Murillo and R. A. Walton, *Multiple Bonds Between Metal Atoms*, Springer Science and Business Media, Inc., New York, 3rd edn, 2005; (*c*) J. F. Berry, in *Metal–Metal Bonding*, ed. G. Parkin, 2010, vol. 136, pp. 1–28; (*d*) S.-A. Hua, Y.-C. Tsai and S.-M. Peng, *J. Chin. Chem. Soc.*, 2014, **61**, 9–26.

4 (*a*) C.-H. Chien, J.-C. Chang, C.-Y. Yeh, G.-H. Lee, J.-M. Fang and S.-M. Peng, *Dalton Trans.*, 2006, 2106–2113; (*b*) C.-K. Kuo, I. P.-C. Liu, C.-Y. Yeh, C.-H. Chou, T.-B. Tsao, G.-H. Lee and S.-M. Peng, *Chem. – Eur. J.*, 2007, **13**, 1442–1451; (*c*) W.-Z. Wang, R. H. Ismayilov, G.-H. Lee, I. P.-C. Liu, C.-Y. Yeh and S.-M. Peng, *Dalton Trans.*, 2007, 830–839; (*d*) M. Nippe and J. F. Berry, *J. Am. Chem. Soc.*, 2007, **129**, 12684–12685; (*e*) M. Ohashi, A. Shima, T. Rüffer, H. Mizomoto, Y. Kaneda and K. Mashima, *Inorg. Chem.*, 2007, **46**, 6702–6714; (*f*) M. Nippe, E. Victor and J. F. Berry, *Eur. J. Inorg. Chem.*, 2008, 5569–5572; (*g*) W.-Z. Wang, R. H. Ismayilov, R.-R. Wang, Y.-L. Huang, C.-Y. Yeh, G.-H. Lee and S.-M. Peng, *Dalton Trans.*, 2008, 6808–6816; (*h*) C. Yin, G.-C. Huang, C.-K. Kuo, M.-D. Fu, H.-C. Lu, J.-H. Ke, K.-N. Shih, Y.-L. Huang, G.-H. Lee, C.-Y. Yeh, C.-h. Chen and S.-M. Peng, *J. Am. Chem. Soc.*, 2008, **130**, 10090–10092; (*i*) R. H. Ismayilov, W.-Z. Wang, R.-R. Wang, Y.-L. Huang, C.-Y. Yeh, G.-H. Lee and S.-M. Peng, *Eur. J. Inorg. Chem.*, 2008, 4290–4295; (*j*) G.-C. Huang, I. P.-C. Liu, J.-H. Kuo, Y.-L. Huang, C.-Y. Yeh, G.-H. Lee and S.-M. Peng, *Dalton Trans.*, 2009, 2623–2629; (*k*) I. P.-C. Liu, C.-H. Chen, C.-F. Chen, G.-H. Lee and S.-M. Peng, *Chem. Commun.*, 2009, 577–579; (*l*) C.-W. Yeh, I. P.-C. Liu, R.-R. Wang, C.-Y. Yeh, G.-H. Lee and S.-M. Peng, *Eur. J. Inorg. Chem.*, 2010, 3153–3159; (*m*) K. Pal, K. Nakao and K. Mashima, *Eur. J. Inorg. Chem.*, 2010, 5668–5674; (*n*) M. Nippe, J. Wang, E. Bill, H. Hope, N. S. Dalal and J. F. Berry, *J. Am. Chem. Soc.*, 2010, **132**, 14261–14272; (*o*) B. S. Dolinar and J. F. Berry, *Inorg. Chem.*, 2013, **52**, 4658–4667; (*p*) D. W. Brogden and J. F. Berry, *Inorg. Chem.*, 2014, **53**, 11354–11356; (*q*) M.-J. Huang, S.-A. Hua, M.-D. Fu, G.-C. Huang, C. Yin, C.-H. Ko, C.-K. Kuo, C.-H. Hsu, G.-H. Lee, K.-Y. Ho, C.-H. Wang, Y.-W. Yang, I.-C. Chen, S.-M. Peng and C.-h. Chen, *Chem. – Eur. J.*, 2014, **20**, 4526–4531; (*r*) D. W. Brogden, J. H. Christian, N. S. Dalal and J. F. Berry, *Inorg. Chim. Acta*, 2015, **424**, 241–247; (*s*) B. S. Dolinar and J. F. Berry, *Polyhedron*, 2016, **103**, 71–78.

5 B. S. Dolinar and J. F. Berry, *Dalton Trans.*, 2014, **43**, 6165–6176.

6 F. H. Allen, *Acta Crystallogr., Sect. B: Struct. Sci.*, 2002, **58**, 380–388.

7 R. D. Shannon, *Acta Crystallogr., Sect. A: Cryst. Phys., Diffr., Theor. Gen. Cryst.*, 1976, **32**, 751–767.